

Rainfall limit of the N cycle on Earth

Stephanie A. Ewing,^{1,2} Greg Michalski,³ Mark Thiemens,⁴ Richard C. Quinn,⁵ Jennifer L. Macalady,⁶ Steven Kohl,⁷ Scott D. Wankel,^{8,9} Carol Kendall,⁸ Christopher P. McKay,¹⁰ and Ronald Amundson¹

Received 9 September 2006; revised 6 April 2007; accepted 23 May 2007; published 8 August 2007.

[1] In most climates on Earth, biological processes control soil N. In the Atacama Desert of Chile, aridity severely limits biology, and soils accumulate atmospheric NO_3^- . We examined this apparent transformation of the soil N cycle using a series of ancient Atacama Desert soils (>2 My) that vary in rainfall (21 to <2 mm yr⁻¹). With decreasing rainfall, soil organic C decreases to 0.3 kg C m⁻² and biological activity becomes minimal, while soil NO_3^- and organic N increase to 4 kg N m⁻² and 1.4 kg N m⁻², respectively. Atmospheric NO_3^- ($\Delta^{17}\text{O} = 23.0\%$) increases from 39% to 80% of total soil NO_3^- as rainfall decreases. These soils capture the transition from a steady state, biologically mediated soil N cycle to a dominantly abiotic, transient state of slowly accumulating atmospheric N. This transition suggests that oxidized soil N may be present in an even more arid and abiotic environment: Mars.

Citation: Ewing, S. A., G. Michalski, M. Thiemens, R. C. Quinn, J. L. Macalady, S. Kohl, S. D. Wankel, C. Kendall, C. P. McKay, and R. Amundson (2007), Rainfall limit of the N cycle on Earth, *Global Biogeochem. Cycles*, 21, GB3009, doi:10.1029/2006GB002838.

1. Introduction

[2] The Atacama Desert of northern Chile contains the world's largest NO_3^- deposits, prompting more than a century of speculation about their origin [e.g., Darwin, 1909; Ericksen, 1981]. Isotopic analysis of commercial grade NO_3^- ores indicates that much of the NO_3^- is atmospheric [Böhlke et al., 1997; Michalski et al., 2004]. Although aridity clearly preserves soluble salts in these soils [Ewing et al., 2006], the specific relationship between rainfall and the regionally variable persistence of atmospheric NO_3^- remains poorly known [Rech et al., 2006]. Globally, about 7% of Earth's land surface is hyperarid [Millenium Ecosystem Assessment, 2005], and 97% of that

area is located in northern Africa, the Arabian peninsula, and western China and Mongolia. However, to our knowledge, NO_3^- rich soils are for the most part unique to northern Chile. We designed this study to examine the effect of rainfall on N cycling and the preservation of atmospheric NO_3^- in soils of the Atacama Desert.

1.1. Soil N and Climate

[3] Soil N inventories and transformations vary strongly with climate [Amundson et al., 2003]. Observations in humid to arid environments have shown that soil N storage decreases with decreasing mean annual rainfall [Jenny and Leonard, 1934; Post et al., 1985]. In biologically active soils, including most deserts, soil N is mostly present in organic forms (>99%), and N storage approaches a steady state between inputs and losses. Inorganic N (IN) consists of relatively small and highly dynamic NO_3^- and NH_4^+ pools, which serve as a supply of "bioavailable" N (Figure 1a).

[4] The shift from biotic desert soils with low N inventories and active N cycling to hyperarid soils with large inventories of accumulated NO_3^- suggests a fundamental change in N dynamics. This dry extreme of the climate spectrum has not been examined by research on the effect of rainfall on soil N [Amundson et al., 2003; Jenny, 1941]. For this study, we selected soils along a natural rainfall gradient in the Atacama Desert, from arid conditions supporting plants to extreme hyperarid conditions lacking plants. We combined soil and atmospheric N measurements with analyses of stable isotopes, radiocarbon, and microbial biomass, to understand how severely limited rainfall, and thus soil biology, transforms the terrestrial N cycle. These observations can help to predict

¹Division of Ecosystem Sciences, Department of Environmental Science Policy and Management, University of California, Berkeley, California, USA.

²Now at Center of Isotope Geochemistry, Department of Earth and Planetary Science, University of California, Berkeley, California, USA.

³Department of Earth and Atmospheric Sciences, Purdue University, West Lafayette, Indiana, USA.

⁴Division of Physical Sciences, University of California, San Diego, La Jolla, California, USA.

⁵SETI Institute, NASA Ames Research Center, Moffett Field, California, USA.

⁶Penn State Astrobiology Research Center, Department of Geosciences, Pennsylvania State University, University Park, Pennsylvania, USA.

⁷Division of Atmospheric Sciences, Desert Research Institute, Reno, Nevada, USA.

⁸U.S. Geological Survey, Menlo Park, California, USA.

⁹Now at Department of Organismal and Evolutionary Biology, Harvard University, Cambridge, Massachusetts, USA.

¹⁰NASA-Ames Research Center, Moffett Field, California, USA.

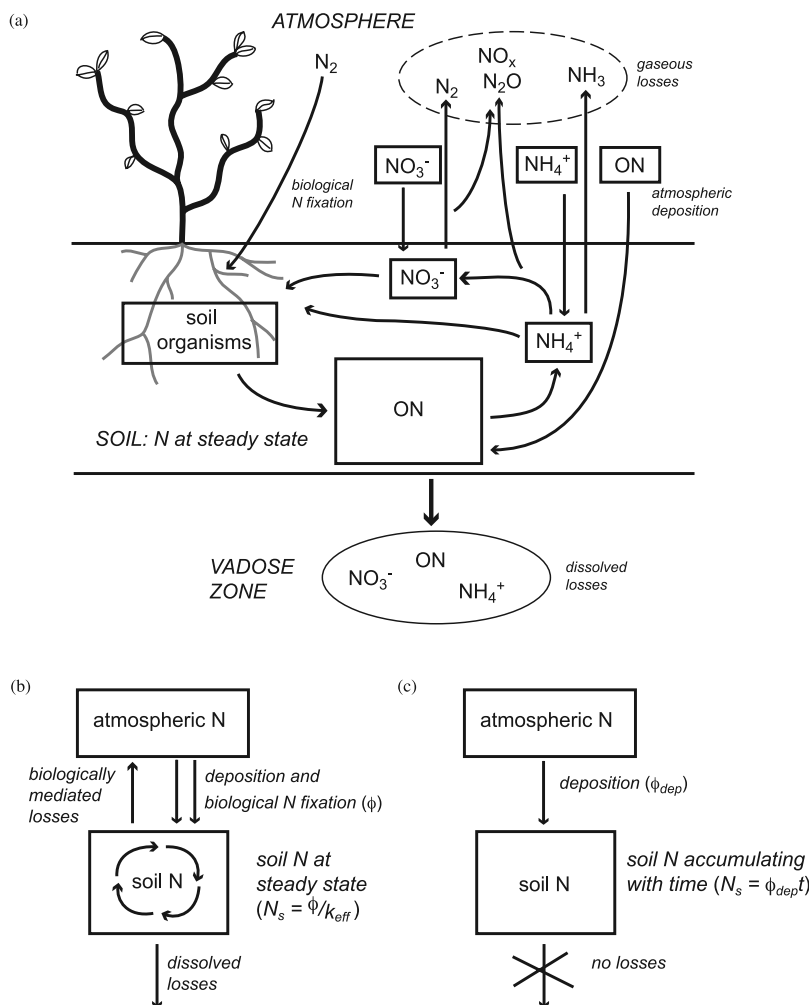


Figure 1. (a) Detailed soil N cycle in most climates; (b) soil N cycle in most climates simplified as inputs and losses; and (c) hypothesized hyperarid soil N “cycle” simplified as inputs only.

whether oxidized N should be present in the more arid and abiotic soils on Mars.

1.2. Model of Soil N Cycle

[5] Rainfall affects the soil N inventory by regulating rates of inputs and losses [Amundson *et al.*, 2003] (Figure 1a). N is added to soils as NO_3^- , NH_4^+ , and organic N (ON) in atmospheric deposition, and by biological N fixation (BNF), at rates that vary spatially and temporally [Cleveland *et al.*, 1999; Galloway *et al.*, 2004; Holland *et al.*, 1999; Neff *et al.*, 2002]. Globally, atmospheric IN deposition has dramatically increased in the last 150 years owing to human activity [Galloway *et al.*, 2004; Holland *et al.*, 1999], although pre-industrial rates of BNF and IN deposition are thought to have been comparable in southern hemisphere deserts [Cleveland *et al.*, 1999; Holland *et al.*, 1999].

[6] Losses of soil N occur as dissolved or gas phase fluxes (Figure 1a). In deserts, NO_3^- leaching is a major form of soil N loss [Walvoord *et al.*, 2003], and gas phase N losses can also be significant with pulsed wetting events [Austin *et al.*, 2004]. Gaseous losses of NO and N_2O

primarily occur during biologically mediated processes (nitrification and denitrification [Firestone and Davidson, 1989]; mineralization [Stark *et al.*, 2002]). NH_3 volatilization is an abiotic loss process that occurs in desert soils at $pH > 7$ [e.g., Schaeffer and Evans, 2005; Schlesinger and Peterjohn, 1991].

[7] Thus for a biologically active plant-soil system (Figure 1a), the balance of N inputs and losses control the soil N inventory (Figure 1b). If inputs are constant (ϕ_N , $\text{mol N m}^{-2} \text{ yr}^{-1}$) and losses are first order, the inventory of soil N (N_s , mol m^{-2}) approaches steady state (inputs = losses) on timescales of 10^3 yr [Brenner *et al.*, 2001]:

$$N_s = \frac{\phi_N}{k_{eff}}, \quad (1)$$

where k_{eff} is a first-order loss constant (yr^{-1}) and $k_{eff}N_s$ is the loss rate ($\text{mol N m}^{-2} \text{ yr}^{-1}$).

[8] We expected that with decreasing rainfall and biological activity, soil N losses would decrease to near-zero levels, and BNF would be negligible (Figure 1c) [Amundson

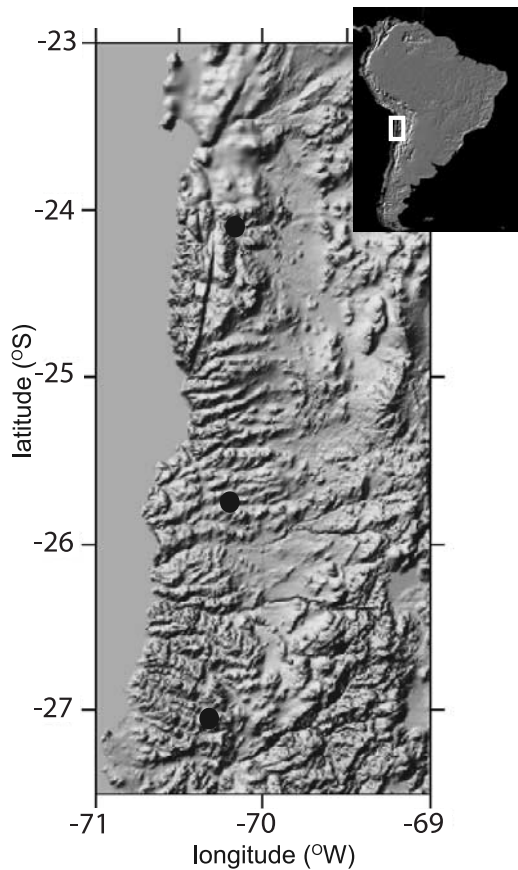


Figure 2. Site locations. Northern site is Yungay (<2 mm rain yr^{-1}), middle site is Altamira (~ 10 mm rain yr^{-1}), and southern site is Copiapó (~ 20 mm rain yr^{-1}).

et al., 2003]. With continuous inputs, the soil N inventory should increase with time (t ; Figure 1c),

$$N_s(t) = \phi_{N,dep}t, \quad (2)$$

where $\phi_{N,dep}$ is atmospheric N deposition. Given minimal biological activity, soil N storage should directly reflect the composition and rate of atmospheric deposition.

[9] In this work, we tested whether hyperarid soils approach this theoretical end-member. By selecting sites that vary from sparse but continuous plant cover to a total absence of plants, we sought to capture the transition between the biologically active, steady state case and the abiotic, nonsteady state extreme. We hypothesized that (1) inputs to all sites should be similar, (2) in-soil transformations and losses control differences among sites, and (3) the driest site retains long-term atmospheric N deposition (equation (2)).

2. Methods

2.1. Study Sites and Sampling

[10] We established three study sites at latitudes ranging from 27°S to 24°S (Figure 2). These sites represent a

rainfall gradient from 21 to <2 mm yr^{-1} [Warren-Rhodes *et al.*, 2006], and a transition from arid to hyperarid climate conditions (“hyperarid” is defined as mean annual precipitation (MAP)/potential evapotranspiration (PET) < 0.05 [see Ewing *et al.*, 2006]). Sites were chosen to minimize differences other than rainfall and the resulting plant communities [Ewing *et al.*, 2006]. Small shrubs form a sparse cover at the arid site, occur in select landscape positions at the intermediate site, and are completely absent at the driest site. The age of the driest soil (Yungay) is between 1.9 and 2.1 My; the two southern sites are >2 My [Ewing *et al.*, 2006].

[11] Soils were excavated to depths of ~ 2 m and sampled by horizon. At each site, combined wet and dry atmospheric deposition was sampled using passive collectors [Reheis and Kihl, 1995], as described previously [Ewing *et al.*, 2006]. Two to three collectors near each site were retrieved after ~ 1 year intervals in 2003, 2004 and 2006. Fog water samples were also collected at the two drier sites in February 2004, as fog wetted soils and plants, and condensate from a small passive fog sampler. Fog samples were frozen in sealed vials for water isotope analysis.

[12] In October 2002, total suspended airborne particles were collected at each site, and in February 2004, sized particles were collected using cascade impactors at the intermediate site and at a coastal site, as described previously [Ewing *et al.*, 2006]. Near the driest site in 2004 and 2005, we also collected airborne particles for OC analysis using stainless steel sampling units (SKC, Inc.), battery operated pumps (BGI, Inc.; 9.0 L min^{-1} ; >100 hours sampling time), and paired quartz filters. Three replicate sample sets and multiple blanks were collected at each site. Sampling occurred through fog events, and likely resulted in collection of fog droplets in addition to airborne particles.

2.2. Analytical Methods

[13] Soil samples were sieved to separate the <2 mm fraction. Total C and N were determined by automated combustion-C-C analysis. Water-soluble salts were extracted by $20\times$ dilution with both distilled deionized (DDI) water and 2M KCl (to ensure complete extraction of NH_4^+). The resulting slurry was filtered (0.2 μm PES) and the filtrate analyzed for NO_3^- and NH_4^+ using automated colorimetry.

[14] OC concentrations and OC- $\Delta^{14}\text{C}$ values were determined using sealed tube combustion, following acidification to remove carbonate, as described previously [Ewing *et al.*, 2006]. Graphitization of purified CO_2 and subsequent analysis was done at the Lawrence Livermore National Laboratory Center for Accelerator Mass Spectrometry for most samples. The $\delta^{13}\text{C}$ value of the CO_2 in all samples, and the $\Delta^{14}\text{C}$ value in 13 samples, were determined at UC Irvine’s Keck Carbon Cycle Accelerator Mass Spectrometry Laboratory facility. The long-term accuracy and precision (1σ) of this technique on modern C ($\Delta^{14}\text{C} > 0\text{‰}$) is $<9\text{‰}$ [Vogel *et al.*, 1984].

[15] NO_3^- was extracted (DDI) and purified from soil and deposition samples containing 10 – 100 μmol NO_3^- and converted to AgNO_3 [Michalski *et al.*, 2004]. The O_2 released upon thermal decomposition was analyzed on a

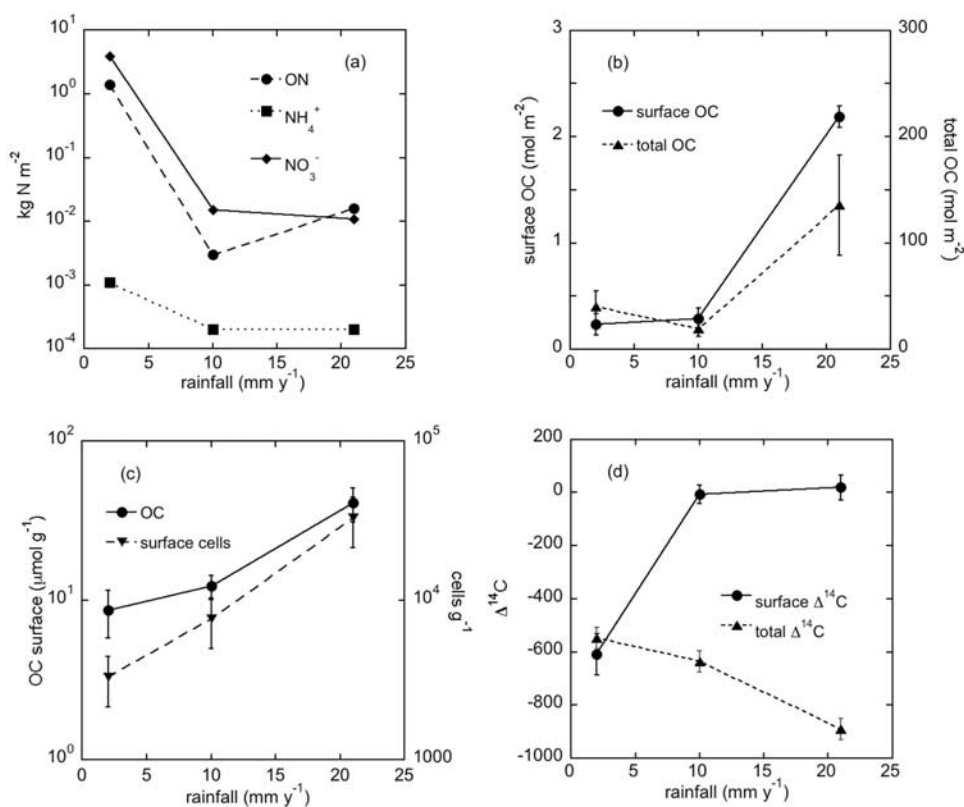


Figure 3. Soil C and N with increasing latitude (increasing rain): (a) soil N pools, (b) surface and total organic C, (c) surface organic C and microbial biomass, and (d) surface and total radiocarbon ($\Delta^{14}\text{C}$).

Finnigan Mat 251 isotope ratio mass spectrometer at UC San Diego [Michalski *et al.*, 2002] (long-term precision for $\delta^{18}\text{O} \pm 2.0\text{‰}$; $\Delta^{17}\text{O} \pm 0.2\text{‰}$; values relative to VSMOW). $\Delta^{17}\text{O}$ values were calculated as $\delta^{17}\text{O} - 0.52 \delta^{18}\text{O}$.

[16] For analysis of $\delta^{15}\text{N}$ and $\delta^{18}\text{O}$ in NO_3^- , $\sim 1 \mu\text{mol NO}_3^-$ was extracted (DDI) from ground soil and analyzed [Sigman *et al.*, 2001; Casciotti *et al.*, 2002] at the USGS stable isotope laboratory in Menlo Park, California, using the bacterial strain *Pseudomonas aureofaciens* (long-term precision: $\delta^{15}\text{N}_{\text{air}} \pm 0.3\text{‰}$, $\delta^{18}\text{O}_{\text{VSMOW}} \pm 0.8\text{‰}$).

[17] Surface horizons were separately sampled for polar lipid fatty acid (PLFA) analysis. Samples were frozen (-20°C) upon collection in Chile, kept on dry ice during transport back to the lab, kept frozen (-20°C) prior to analysis, and processed within one week. Ten to 15 replicate 30-g extractions were made for each sample and pooled, so that the final pooled mass of soil analyzed was 300 to 500 g. PLFAs were extracted and purified as described previously [Macalady *et al.*, 2002], and analyzed by gas chromatography-mass spectrometry (GC-MS) in the lab of T. Torok at Lawrence Berkeley National Laboratory. Peaks were identified using 33 bacterial FAME standards and MIDI peak identification software (Microbial ID Inc., Newark, Delaware) integrated with the GC-MS system. Microbial biomass was estimated by assuming 2.2×10^7 PLFA molecules/cell.

[18] Soluble salts were extracted from deposition traps and filters as described previously [Ewing *et al.*, 2006]. Air and deposition samples were analyzed by the Desert Re-

search Institute in Reno, NV using IC (NO_3^-) and automated colorimetry (NH_4^+). Organic and elemental C analysis at the University of Wisconsin, Madison, used stepped heating/pyrolysis [Schauer *et al.*, 2003].

[19] Water was extracted from fog-wetted samples by cryogenic distillation for one hour under vacuum [West *et al.*, 2006]. The stable O isotopic composition of distilled samples was determined on an isotope ratio mass spectrometer (Finnigan Mat Delta^{plus} XL, Germany) at the UC Berkeley Center for Stable Isotope Biogeochemistry (versus VSMOW; long-term precision of 0.11‰ using two internal standards traceable to IAEA standards).

3. Results and Discussion

3.1. Soil N With Decreasing Rainfall

[20] The soil N inventory increases sharply with the transition from arid to extreme hyperarid conditions (Figure 3a). This increase is contrary to the decrease in soil N observed at humid to semiarid sites [Post *et al.*, 1985]. With decreasing rainfall, the character of soil N also changes: 88% organic at the arid site, 22% organic at the intermediate site, and 28% organic at the driest site.

[21] The arid soil has a functioning ecosystem and conforms to the expected pattern for biologically active soils with arid conditions. Its soil N inventory (0.029 kg m^{-3}) is dominated by ON, but is among the lowest reported for soils [Post *et al.*, 1985]. The more hyperarid sites represent a departure from previous observations of soil N versus

climate. Total N is high, and dominated by NO_3^- . The accumulation of NO_3^- with declining rainfall is consistent with the abiotic extreme (equation (2)) in which deposition is preserved. Given this trend in NO_3^- , the low levels of NH_4^+ in all soils (0.2 to 1.1 g N m⁻²) are striking because deposition of NH_4^+ should be comparable to that of NO_3^- (see deposition results in this paper, and Galloway *et al.* [2004]). These low NH_4^+ levels suggest loss either during or after deposition in the soils, including the driest soil where NO_3^- is retained.

[22] The inventory of ON is highest in the driest soil (1.4 kg m⁻²; Figure 3a). This was unanticipated given the near absence of local biological activity [Navarro-Gonzalez *et al.*, 2003; Warren-Rhodes *et al.*, 2006]. This ON storage, if not a fossil reservoir, suggests that atmospheric ON deposition is important, and that decomposition rates are exceedingly low. In the next section, we consider rates of OC cycling provide insight into ON dynamics.

3.2. Soil C Cycling With Decreasing Rainfall

[23] With decreasing rainfall, OC decreases in soil surface horizons (0–2 cm) and in OC inventories to 1 m (Figure 3b), consistent with the larger global trend [Amundson, 2001]. These trends of decreasing OC across the arid-hyperarid transition (Figure 3b) are opposite those of soil N (Figure 3a), suggesting that losses of soil OC are greater relative to inputs than losses of soil N.

[24] We used the PLFA assay in surface horizons (upper 1 to 2 cm) to provide an estimate of the microbial biomass that would have immediate access to OC deposited from the atmosphere. These data indicate that the microbial biomass in surface horizons drops from 10⁵ cells g⁻¹ in the arid soil to 10³ cells g⁻¹ in the driest soil (Figure 3c). These values are orders of magnitude lower than the average of 10⁹ cells g⁻¹ in most soils [Sylvia *et al.*, 1998]. With the transition to extreme hyperaridity, microbial biomass declines precipitously but is still detectable.

[25] PLFA are generally assumed to decompose rapidly in soils [Guckert *et al.*, 1985], making this class of compounds a useful assay of living microorganisms. It could be argued that rapid biological decomposition does not occur at the driest site, and the PLFA data reflect the accumulated residue of dead cells. However, rapid abiotic oxidation of OC compounds has been observed in the Atacama [Quinn *et al.*, 2005], and the PLFA-derived biomass values are consistent with estimates of viable microorganisms at the soil surface using plate counts [Navarro-Gonzalez *et al.*, 2003]. Moreover, microbial biomass and activity may increase below the upper 2 cm given harsh conditions at the soil surface [Maier *et al.*, 2004]. Therefore the PLFA data likely represent viable biomass, even at the driest site. There an exceedingly small microbial community may survive by virtue of fog/dew events, resulting in a slow or highly episodic C cycle.

[26] Organic $\Delta^{14}\text{C}$ values in surface horizons decrease from +7 ± 44‰ (n = 5) at the arid site to -609 ± 77‰ (n = 2) at the driest site (Figure 3d). These values show that apparent rates of C cycling decrease sharply with decreasing rainfall: residence times are decadal or shorter at the arid site, increasing to a modeled mean residence time of

1.3 × 10⁴ years at the driest site (auxiliary material Text S1 equation (4)¹). This apparent rate in the driest region is the slowest observed for a soil surface horizon [Amundson, 2001; Trumbore, 2000].

[27] In the arid soil, the depth-integrated soil $\Delta^{14}\text{C}$ value (-890‰) is considerably lower than that of the surface horizon (+7‰), indicating that C cycling is focused at the soil surface, as expected for vegetated sites (Figure 3d). In the driest soil, the depth integrated soil $\Delta^{14}\text{C}$ value (-550‰) is equal within error to the surface horizon value (-609 ± 77‰) (Figure 3d), revealing an apparent lack of variation in OC cycling with depth. However, the OC is not radiocarbon “dead” (-996‰), indicating slow C turnover (auxiliary material Text S1 equation (8)).

[28] On the basis of the depth-integrated soil $\Delta^{14}\text{C}$ value in the driest soil (-550‰), the steady state OC input rate is 1700 μmol m⁻² yr⁻¹ (auxiliary material Text S1 equations (2)–(4)). This apparent rate, when compared to total long-term salt deposition (0.4 g m⁻² yr⁻¹ [Ewing *et al.*, 2006]) suggests that OC has been 5% of salt inputs, consistent with reported OC concentrations in marine aerosols (1 to 19% [Hoffman and Duce, 1974]). Given the evidence of a small but viable microbial biomass, these results suggest that slow biological decomposition of marine derived organic matter has occurred. Thus while substantial ON has been preserved in this soil, a fraction has likely been mineralized during decomposition.

3.3. C and N in Airborne Particles and Deposition

[29] We measured atmospheric C and N directly, in order to demonstrate that the rate and character of inputs are similar among sites. The solute inventories in the driest soil also provide a measure of long-term atmospheric N accumulation that should most closely resemble inputs [Ewing *et al.*, 2006]. By comparing inputs with accumulation in the driest soil, we can begin to identify whether N transformation occurs with extreme hyperaridity.

3.3.1. Atmospheric Inorganic N

[30] In October 2002, airborne NO_3^- and NH_4^+ concentrations were relatively consistent among sites and similar to each other at a given site (Figure 4a). In three years of samples, NO_3^- deposition rates exceeded those of NH_4^+ by about an order of magnitude (Figure 4b). While this difference may reflect some degree of seasonal variation, it may also occur because NO_3^- is present on larger particles that are more readily deposited at the land surface. In airborne particles, NO_3^- was detected in particles 2.5–12 μm in diameter (5.9 ± 3.4 nmol m⁻³, n = 3), and 0.5–2.5 μm in diameter (3.6 ± 1.3 nmol m⁻³, n = 4), while 99% of NH_4^+ was in particles <0.5 μm (35.0 ± 4.9 nmol NH₄⁺ m⁻³, n = 4).

[31] NO_3^- deposition averaged 3.3 ± 0.8 mmol m⁻² yr⁻¹ (n = 3 sites). A lower long-term deposition rate can be calculated from the inventory and age of the driest soil (0.13 mmol m⁻² yr⁻¹ [Ewing *et al.*, 2006]; see auxiliary material Text S1 equation (9)). This long-term rate is also an order of magnitude less than both modeled rates of pre-

¹Auxiliary materials are available in the HTML. doi:10.1029/2006GB002838.

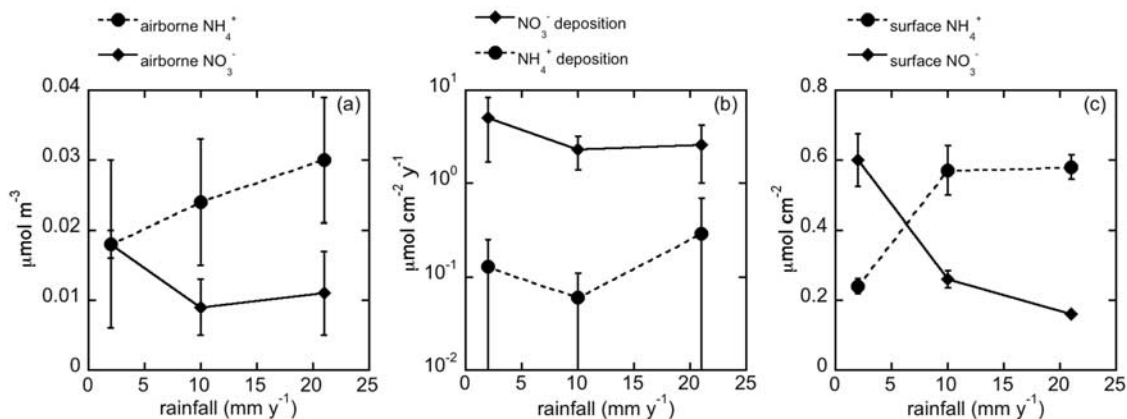


Figure 4. NO_3^- and NH_4^+ with increasing latitude (increasing rain) in (a) atmosphere (October 2002), (b) combined wet and dry deposition to passive traps (2002–2006; $n = 3$), and (c) surface soil (1–2 cm depth).

industrial NO_3^- deposition in southern hemisphere deserts (1.4 to 5.6 $\text{mmol m}^{-2} \text{yr}^{-1}$ [Holland *et al.*, 1999]) and a previous estimate for this region (1.2 $\text{mmol m}^{-2} \text{yr}^{-1}$ [Michalski *et al.*, 2004]). However, given uncertainties in both modeled pre-industrial values and our short-term contemporary deposition observations, the soil-based NO_3^- deposition rate is a useful conservative estimate of the long-term rate of NO_3^- deposition [Ewing *et al.*, 2006]. While short-term deposition rates were higher, they were relatively consistent among sites, suggesting that differences in atmospheric deposition do not explain the soil N chemistry differences.

[32] NH_4^+ deposition averaged $160 \pm 70 \mu\text{mol m}^{-2} \text{yr}^{-1}$ ($n = 3$ sites). Long-term NH_4^+ deposition can be estimated on the basis of the observation that it is primarily associated with SO_4^{2-} in air samples [Ewing *et al.*, 2006]. As with NH_4^+ , most SO_4^{2-} (83%) in airborne samples was in particles $<0.5 \mu\text{m}$; NH_4^+ was the apparent counter-ion for 50% of SO_4^{2-} in particles $<0.5 \mu\text{m}$, and 5% of SO_4^{2-} in particles 0.5–12 μm (more readily deposited). Applying this range to the soil-based SO_4^{2-} deposition rate (1.4 mmol S m^{-2} [Ewing *et al.*, 2006]) the long-term NH_4^+ deposition rate is 70 to 700 $\mu\text{mol m}^{-2} \text{yr}^{-1}$, comparable to the short-term rate. Compared with the NH_4^+ storage of the driest soil (0.04 $\mu\text{mol m}^{-2} \text{yr}^{-1}$), this implies that 99.9% of deposited NH_4^+ has been lost or transformed.

[33] A loss or transformation of NH_4^+ is further indicated by a comparison of airborne, deposition, and soil $\text{NH}_4^+/\text{NO}_3^-$

mole ratios (Table 1). This ratio is highest in airborne particles (1.0), intermediate in deposition trap and driest surface horizon samples (0.05 and 0.15, respectively) and lowest in the driest soil inventory (0.0004) (Table 1). This suggests that NH_4^+ is deposited to soils but is continuously transformed or lost, possibly via NH_3 volatilization [Ewing *et al.*, 2006].

3.3.2. Atmospheric Organic C and N

[34] The average OC in airborne samples was $0.46 \pm 0.18 \mu\text{g m}^{-3}$ ($n = 2$ years), and elemental C exceeded uncertainty in 2005 ($0.13 \pm 0.09 \mu\text{g m}^{-3}$, $n = 2$ samples) but not in 2004. This amount of OC is $7 \pm 3\%$ of total airborne salts at all sites in 2002 ($7 \pm 1 \mu\text{g m}^{-3}$; $n = 9$ [Ewing *et al.*, 2006]), consistent with typical marine aerosols (1–19% [Hoffman and Duce, 1974]), and our earlier estimate (5% of total salts).

[35] It is likely that ON is deposited with OC. Our detection of elemental C, a combustion product, suggests an anthropogenic component in our air samples. However, the presence of substantial ON in the driest soil indicates long-term, nonanthropogenic deposition of airborne ON and OC. The long-term, soil-based ON accumulation rate is 50 $\mu\text{mol m}^{-2} \text{yr}^{-1}$, but total deposition may be higher. Two independent estimates of total ON deposition indicate ON transformation following deposition: (1) the steady state OC input rate (1700 $\mu\text{mol m}^{-2} \text{yr}^{-1}$), divided by observed OC/ON ratios in atmospheric samples (2:1 to 20:1 [Cornell *et al.*, 2003]) and (2) typical

Table 1. Airborne Concentrations, Fluxes, and Driest Soil Inventories of C and N

	Airborne, $\mu\text{mol m}^{-3}$	Measured Deposition, $\mu\text{mol m}^{-2} \text{yr}^{-1}$	Soil-Based Deposition, $\mu\text{mol m}^{-2} \text{yr}^{-1}$	Soil-Based Deposition Velocity, cm s^{-1}	Yungay Surface (0–2 cm), mol m^{-2}	Yungay inventory (0–1 m), mol m^{-2}
NH_4^+	0.0181	160	0.04 (400) ^a	6E-6	0.004	0.110
NO_3^-	0.0182	3300	133	0.02	0.027	255
$\text{NH}_4^+/\text{NO}_3^-$	1	0.05	(3)		0.15	0.0004
ON	~0.01		48 (250)	0.02	0.199	100
OC	0.038		(1700)	0.14	0.232	40
OC/ON	2–20		(23)		1	0.4

^aParentheses denote estimated rather than directly measured values, as discussed in text.

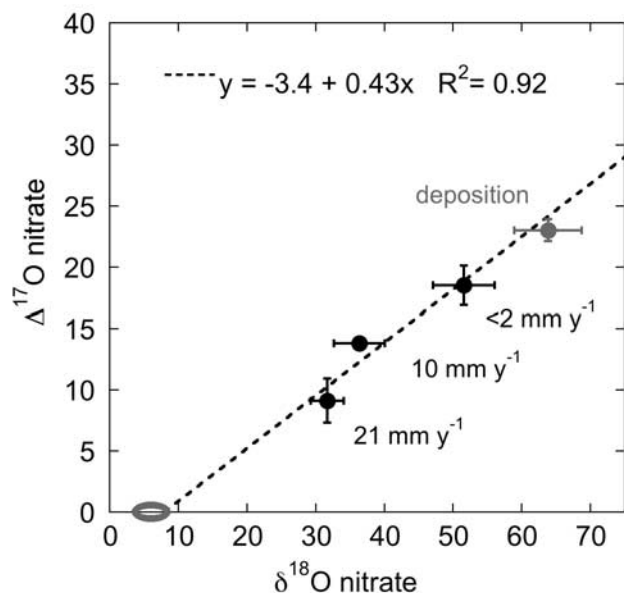


Figure 5. NO_3^- - $\delta^{18}\text{O}$ versus $\Delta^{17}\text{O}$ at all sites (depth-weighted mean value for each site) and in atmospheric deposition. Error bars represent both within-site variability (Table 2) and analytical error. Nonatmospheric nitrate values are based on local water values [Vuille *et al.*, 2003].

proportions of ON in the atmosphere (20–65% of total N [Cornell *et al.*, 2003; Neff *et al.*, 2002]), given the total soil-based IN deposition ($\geq 200 \mu\text{mol m}^{-2} \text{yr}^{-1}$ including estimated NH_4^+ deposition). These estimates suggest that at least 2/3 of the deposited ON (~ 100 – $200 \mu\text{mol m}^{-2} \text{yr}^{-1}$) has been transformed or lost. OC/ON ratios provide further evidence of ON transformation.

3.3.3. OC/ON of Atmosphere Versus Driest Soil

[36] Typically, soil C/N ratios do not decrease below that of the microbial biomass (~ 5). Here soil OC/ON ratios are unusually low, decreasing between the surface soil (OC/ON = 1) and the soil inventory (OC/ON = 0.4) (Table 1). Slow decomposition or transformation over My timescales can explain these low values. Our estimated OC and ON input rates (1700 and $\sim 200 \mu\text{mol m}^{-2} \text{yr}^{-1}$, respectively) indicate an atmospheric OC/ON of ~ 9 . Subtracting the apparent ON accumulation rate in soil ($50 \mu\text{mol m}^{-2} \text{yr}^{-1}$) from the ON input rate, the material transformed would contain $\sim 150 \mu\text{mol ON m}^{-2} \text{yr}^{-1}$ and have an average OC/ON of ~ 11 , only slightly higher than the input value, in order to result in the observed soil OC/ON. We have assumed steady state for OC, and the similar input and loss ratios suggest that steady state is also possible for ON. In general, these unusually low C/N ratios indicate faster transformation of C than N, and if they are the result of biological activity, could signal that this is a C limited system due to water limited photosynthetic activity. Further work is needed to confirm these low ratios and their causes.

3.4. NO_3^- O Isotope Values

[37] The isotopic composition of atmospheric deposition provides an end-member for determining the origin of soil

NO_3^- (auxiliary material Text S1 Appendix 3). NO_3^- collected in the passive deposition collectors at the driest site had an O isotopic composition typical of purely atmospheric NO_3^- : a $\Delta^{17}\text{O}$ value of $23.0 \pm 0.9\text{‰}$ ($n = 3$) and a $\delta^{18}\text{O}$ value of $63.9 \pm 4.9\text{‰}$ ($n = 3$). The $\Delta^{17}\text{O}$ value is close to a global estimate based on common pathways of NO_3^- formation in the atmosphere (24.7‰ [Michalski *et al.*, 2004]), and is consistent with measured values of 20–30‰ observed at coastal and inland sites in southern California [Michalski *et al.*, 2003]. The $\delta^{18}\text{O}$ value ($63.9 \pm 4.9\text{‰}$) is consistent with observed $\delta^{18}\text{O}$ values of 60 to 90‰ for atmospheric NO_3^- in aerosols and remote rain and snow [Hastings *et al.*, 2003, 2004; Michalski *et al.*, 2003]. Our samples reflect a year of combined wet and dry deposition, and therefore represent a seasonally integrated value.

[38] With declining rainfall, the depth-integrated soil NO_3^- - $\Delta^{17}\text{O}$ values increase from 9.1‰ to 18.5‰, approaching our observed atmospheric value (Figure 5). The depth-integrated soil NO_3^- - $\delta^{18}\text{O}$ values increase from 32‰ to 52‰ with decreasing rain, and are linearly correlated with the NO_3^- - $\Delta^{17}\text{O}$ values ($R^2 = 0.92$; Figure 5). This correlation is consistent with a two-component mix between atmospheric NO_3^- ($\Delta^{17}\text{O} = 23 \pm 1\text{‰}$, $\delta^{18}\text{O} = 64 \pm 5\text{‰}$) and NO_3^- produced via in-soil oxidation ($\Delta^{17}\text{O} = 0\text{‰}$, $\delta^{18}\text{O} = 7.9\text{‰}$; Figure 5 regression intercept). The soil NO_3^- - $\Delta^{17}\text{O}$ values indicate an increase in the atmospheric portion of total soil NO_3^- , from 39% at the arid site to 80% at the driest site. At the driest site, the soil NO_3^- - $\Delta^{17}\text{O}$ values fall within the range of values for ore-grade Atacama NO_3^- (13.7 to 21.6‰ [Michalski *et al.*, 2004]). The NO_3^- isotope and concentration data show that the arid-hyperarid transition has two effects: (1) negligible leaching leads to a large, accumulating soil NO_3^- inventory, and (2) reduced biological activity results in greater preservation of the atmospheric O isotope signal. Atmospheric NO_3^- in the driest soil has been preserved unaltered for millions of years.

3.5. In-Soil Sources of Nonatmospheric NO_3^-

[39] On the basis of soil NO_3^- - $\Delta^{17}\text{O}$ values, atmospheric NO_3^- increases with decreasing rainfall, but even at the driest site, 20% of total NO_3^- ($55 \text{ mol NO}_3^- \text{N m}^{-2}$) was produced in situ. This indicates that over 2.1 My, $26 \mu\text{mol N m}^{-2} \text{yr}^{-1}$ has been oxidized to NO_3^- . This rate is seven orders of magnitude lower than microbial nitrification rates in wetter climates [Booth *et al.*, 2005]. Our estimated rate of ON + NH_4^+ transformation (~ 220 – $950 \mu\text{mol m}^{-2} \text{yr}^{-1}$) exceeds this net rate of N oxidation by an order of magnitude. Since the transformation products are not present in the soil, only very small amounts of ON and NH_4^+ may be oxidized to soil NO_3^- . This indicates that much of the ON and most of the NH_4^+ are transformed to gas phase products by biotic or abiotic means, and pass out of the soil.

3.6. Nitrate- $\delta^{15}\text{N}$ and $-\delta^{18}\text{O}$ Values

[40] The soil NO_3^- - $\delta^{15}\text{N}$ values are variable and generally increase with depth, ranging from 0.40 to 8.15‰ in the arid soil, and from -1.96 to $+8.21\text{‰}$ in the driest soil (Figure 6a). This isotopic variation with depth is unlikely to reflect N source changes over time, because the depth

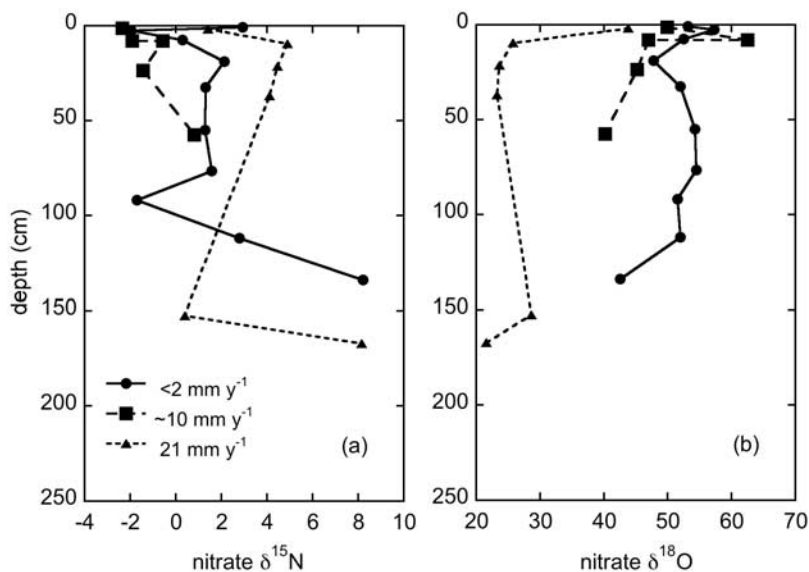


Figure 6. (a) NO_3^- - $\delta^{15}\text{N}$ and (b) NO_3^- - $\delta^{18}\text{O}$ with depth at all sites.

distribution of salts indicates that NO_3^- has been mixed and concentrated at depth by episodes of wetter conditions in the past [Ewing *et al.*, 2006]. This suggests that in-soil processes drive the observed variation.

[41] Soil NO_3^- - $\delta^{15}\text{N}$ values are inversely correlated with $\delta^{18}\text{O}$ values (Figure 7). This could indicate dilution of atmospheric NO_3^- by soil NO_3^- that is ^{15}N -enriched and ^{18}O -depleted relative to atmosphere, but in that case a negative correlation between NO_3^- - $\delta^{15}\text{N}$ and NO_3^- - $\Delta^{17}\text{O}$ should result. Our data are sufficient to make this comparison only at the driest site, where no such correlation is apparent (Table 2). In addition, NO_3^- - $\delta^{15}\text{N}$ values are similar among sites (Figure 6), despite the observed variation in O isotopes with rainfall (Figure 5).

[42] The isotopic data require processes that have an inverse effect on $\delta^{15}\text{N}$ and $\delta^{18}\text{O}$ values in NO_3^- without significantly changing the proportion of atmospheric NO_3^- present (i.e., $\Delta^{17}\text{O}$; see auxiliary material Text S1 Appendix 3). This could occur with: (1) mass-dependent fractionation, with downward transport and precipitation of NO_3^- salts, as observed for CaSO_4 minerals [Ewing *et al.*, 2005]; or (2) multiple in situ sources of N in NO_3^- , with different $\delta^{15}\text{N}$ values and oxidation pathways. The first possibility has not been considered before owing to the rarity of solid phase nitrate salts, and we know of no reported fractionation factors for this process. However, observations for S and O in sulfate [Ewing *et al.*, 2005] suggest that dissolution and reprecipitation with downward transport might be expected to favor the lighter isotopes of both N and O; here the heavier N isotope is favored with depth. The second possibility (multiple sources) is consistent with NO_3^- formation from both ON and NH_4^+ if the oxidation pathway (or O source) varies in a species-dependent manner. ON-derived NO_3^- may have a low $\delta^{15}\text{N}$ value because mineralization (or perhaps photolysis; see section 3.7) favors the light isotope, while NH_4^+ -source NO_3^- may be enriched in ^{15}N by NH_3 volatilization. NO_3^- - $\delta^{18}\text{O}$ values may vary with the abundance of NH_4^+

[Mayer *et al.*, 2001]. If ON and NH_4^+ are oxidized at different depths, the oxidizing water may have variable $\delta^{18}\text{O}$ values due to depth-dependent evaporation, resulting in different NO_3^- - $\delta^{18}\text{O}$ values for the two species. Gas phase N losses in addition to NH_3 volatilization would complicate these trends. For example, loss of N oxides would increase both ^{15}N and ^{18}O in the residual NO_3^- .

[43] The relationship between $\delta^{18}\text{O}$ and $\Delta^{17}\text{O}$ at all sites (Figure 5) suggests a nonatmospheric NO_3^- end-member that is formed from water with a $\delta^{18}\text{O}$ value of about 0‰ (auxiliary material Text S1 Appendix 3). Fog water had $\delta^{18}\text{O}$ values of $-3.3 \pm 0.7\text{‰}$ ($n = 7$) and $-5.5 \pm 1.7\text{‰}$ ($n = 7$) at the intermediate and driest sites, respectively. While

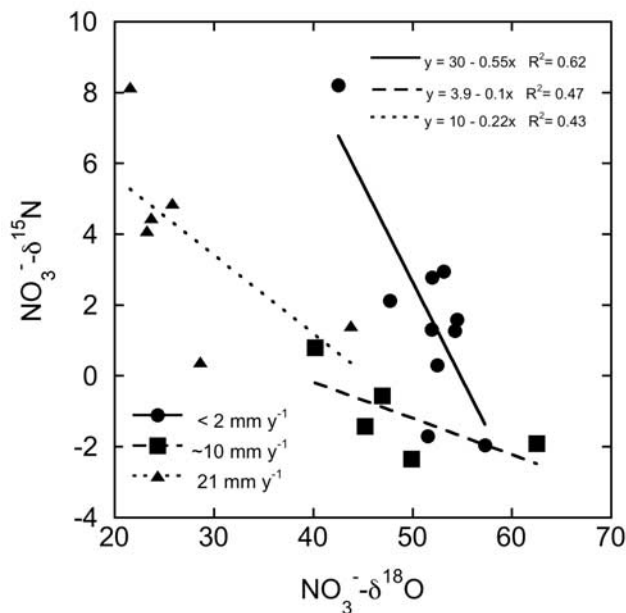


Figure 7. For all sites, $\delta^{18}\text{O}$ versus $\delta^{15}\text{N}$.

Table 2. N and O Isotope Values of NO_3^- in the Soils Examined in the Study

Site, mm rain yr^{-1}	Soil Depth, cm	NO_3^- - $\delta^{15}\text{N}^{\text{a}}$	NO_3^- - $\delta^{18}\text{O}^{\text{b}}$	NO_3^- - $\delta^{18}\text{O}^{\text{a}}$	NO_3^- - $\Delta^{17}\text{O}^{\text{b}}$	$1 \sigma (\Delta^{17}\text{O})$	n^{c}	% atm ^d
<2	deposition	–	63.9		23.0	0.9	3	100
<2	1	2.94	53.8	53.16	19.5		1	85
<2	3	–1.96	57.3	57.29	19.3		1	84
<2	8	0.29	52.4	52.50	15.3		1	66
<2	19	2.12		47.74				
<2	33	1.30		51.93				
<2	55	1.27	50.1	54.26	18.9	0.7	3	82
<2	77	1.58	52.9	54.49	18.2	0.4	4	79
<2	92	–1.70	50.5	51.56	18.1	0.6	3	79
<2	112	2.78	54.5	51.95	18.3	0.2	4	80
<2	134	8.21	45.2	42.53	17.7	0.2	2	77
<2	150				17.5			76
<2	167		49.7		17.2		1	75
<2	186		50.7		18.2	1.0	4	79
<2	202		50.5		17.3	0.4	4	75
<2	216		49.8		16.8	0.8	2	73
~10	2	–2.35		49.9				
~10	8	–1.91		62.51				
~10	8	–0.57		46.94				
~10	24	–1.43		45.21				
~10	58	0.80		40.21				
~10	89		40.0		14.0	0.1	2	61
~10	106		36.1		13.7		1	60
21	2			43.77				
21	9.5			25.78				
21	21.5			23.66				
21	37			23.24				
21	153		31.0	28.61	9.2		1	40
21	167		31.9	21.55	9.4		1	41

^aDenitrifier method ($\delta^{15}\text{N} \pm 0.3\text{‰}$; $\delta^{18}\text{O} \pm 0.8\text{‰}$).

^bMichalski *et al.* [2002] ($\delta^{18}\text{O} \pm 2.0\text{‰}$; $\Delta^{17}\text{O} \pm 0.2\text{‰}$).

^cLaboratory extraction replicates for triple O isotope analysis.

^dPercentage of total soil NO_3^- that is atmospheric, with 100% = 23.0‰.

controls on the net isotopic values in NO_3^- likely vary across sites, the low fog water values suggest that NO_3^- - $\delta^{18}\text{O}$ values are elevated by either a loss mechanism or by evaporation of soil/fog water prior to its incorporation in nonatmospheric NO_3^- . Further work is needed to fully evaluate these hypotheses, but our data suggest multiple pathways of in situ N transformation, even in the driest soil.

3.7. Transformation of the Soil N Cycle at the Arid-Hyperarid Transition

[44] The arid-hyperarid transition alters the primary processes controlling soil N, and the result is hyperarid soils that are unique on Earth because they are essentially abiotic with respect to N cycling. Inputs to the driest soil by atmospheric N deposition total $\sim 500 \mu\text{mol m}^{-2} \text{yr}^{-1}$ (Figure 8). About a third of this is retained in the soil, resulting in accumulation of a large inventory of unaltered atmospheric NO_3^- and substantial ON over millions of years. Of estimated total N losses from the driest soil ($\sim 300 \mu\text{mol m}^{-2} \text{yr}^{-1}$) at least a third may arise from the abiotic process of NH_3 volatilization (as discussed in section 3.3.1; estimated values in Figure 8). Photolytic transformation of N is also possible at the soil surface [Austin and Vivanco, 2006; Zhang and Anastasio, 2003; Calza *et al.*, 2005], with unknown effects on stable isotope values and N

speciation. Thus much of the hyperarid N cycle revealed by this work (Figure 8) is a function of abiotic processes.

[45] However, our data suggest that even under the most extreme hyperarid conditions on Earth, biological C and N cycling continue to occur at very low levels. Detectable microbial biomass suggests that slow turnover of atmospherically derived OC ($\sim 1700 \mu\text{mol m}^{-2} \text{yr}^{-1}$) is at least partly biotic, and accompanied by slow mineralization of atmospheric ON ($\sim 150 \mu\text{mol m}^{-2} \text{yr}^{-1}$). Low levels of both ON mineralization and nitrification may contribute to the inventory of nonatmospheric NO_3^- in the driest soil, and associated N losses may occur. By virtue of their antiquity, these largely abiotic soils contain evidence suggesting very low levels of biological activity.

3.8. Sources of Atmospheric NO_3^- in Atacama Desert Soils

[46] In the Atacama Desert, the NO_x precursor of NO_3^- has several possible origins, including lightning, stratospheric mixing, biomass burning, local soils and volcanic emissions. The influence of biomass burning is expected to be negligible [Michalski *et al.*, 2004], and the contributions of lightning, mixing, and local soils should be small. The significant quantities of ON in the driest soil may offer an additional clue, as they are unlikely to be derived from

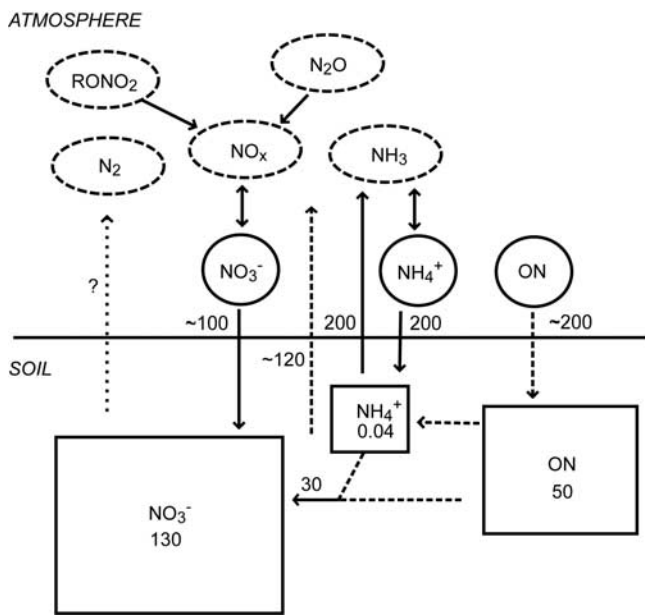


Figure 8. Hyperarid soil N “cycle” based on this work. All units are $\mu\text{mol m}^{-2} \text{yr}^{-1}$. The soil N inventory divided by soil age ($130 \mu\text{mol m}^{-2} \text{yr}^{-1}$) is 26% of estimated inputs ($\sim 500 \mu\text{mol m}^{-2} \text{yr}^{-1}$).

volcanic emissions, and may reflect the influence of highly productive, upwelling waters at the coast of northern Chile [e.g., Moore *et al.*, 2002]. A marine origin is consistent with observations for soil sulfate at sites near the coast [Rech *et al.*, 2003], and formation of sea salt would be expected to entrain ON [Hoffman and Duce, 1974].

[47] With onshore transport, sea salt also serves as a locus of NO_3^- formation from NO_x . A possible mechanism of increased NO_x formation in this region is via photochemical production and sea-air flux of gas phase alkyl nitrate compounds (RONO_2 [Blake *et al.*, 2003; Dahl *et al.*, 2005; Moore and Blough, 2002]). Upwelling waters are high in RONO_2 precursors ($\text{NO}_2^-/\text{NO}_3^-$ and photoreactive organic matter), and once formed, RONO_2 compounds photolyze to form NO_x , over timescales of days to weeks [Blake *et al.*, 2003; Dahl *et al.*, 2005]. Thus they serve as a means of transforming dissolved $\text{NO}_2^-/\text{NO}_3^-$ in the water column to a NO_x reservoir that may then be transported onshore and deposited as NO_3^- . Maximum CH_3ONO_2 concentrations have been observed in the equatorial Pacific (~ 50 pptv), with short residence times suggesting transport rates exceeding those of photolysis [Blake *et al.*, 2003]. While this hypothesis remains to be tested by future work, we suggest that the unique NO_3^- deposits of the Atacama Desert may reflect photochemical mobilization of upwelling marine $\text{NO}_2^-/\text{NO}_3^-$.

3.9. Implications for Mars Regolith

[48] Planetary atmospheres bear the signature of chemical processes integrated over geologic timescales. Earth’s N_2 rich atmosphere is maintained through biological denitrification, returning reduced N to its largest reservoir. It has been proposed [Capone *et al.*, 2006] that the absence of life

would break this cycle, depleting the atmospheric reservoir and storing oxidized N in surface or deeper reservoirs.

[49] The Atacama Desert is as close to an ancient abiotic environment as can be found on Earth, and has been proposed as an analog for Mars research [Navarro-Gonzalez *et al.*, 2003; Quinn *et al.*, 2005]. This work shows that extreme aridity stalls the N cycle by limiting biology, resulting in soils that store oxidized N. During the past on Mars, volcanism, meteor shock and lightning may have produced fixed N as NO and HCN [Segura and Navarro-González, 2005]. While the oxidizing capacity of the Martian atmosphere over time is debatable, the current presence of SO_4^{2-} in soils is testament to oxidation processes. The relatively low N_2 content of the Martian atmosphere may partly reflect NO_3^- storage in Martian soils.

4. Conclusions

[50] The substantial accumulation of NO_3^- in the Atacama Desert is a consequence of the near-cessation of the soil N cycle as we know it on Earth. Biology is not absent from the most hyperarid Atacama Desert soils, yet its limited influence makes them largely abiotic with respect to elemental cycles of fundamental importance to life. Because severely limited rainfall restricts leaching and biology, it is atmospheric N deposition, rather than microbial transformation, that controls N inventories and speciation. Thus the arid-hyperarid transition represents a threshold in the relationship between soil N and rainfall on Earth (Figure 9).

[51] At the same time, this work shows that N losses continue to occur under extreme hyperarid conditions, most likely as gas phase products (NH_3 , NO_x , N_2O) of both biotic and abiotic N transformations (Figure 8). Upon transport out of the soil, the more reactive species (NH_3 , NO_x) will be transformed to particle phase N in the atmosphere and redeposited regionally. In this sense hyperaridity short-circuits the soil N cycle, shifting the balance of N transformations toward the soil surface and atmosphere, where

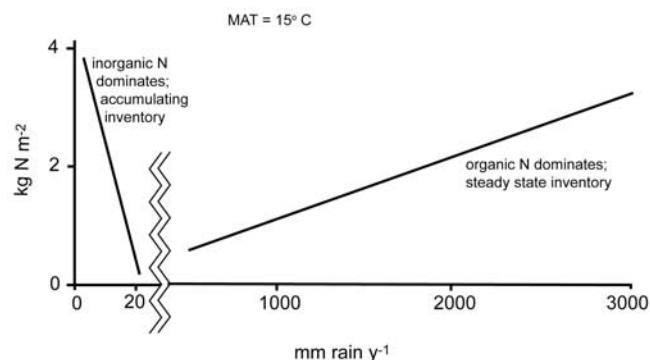


Figure 9. Schematic of trends in soil N with rainfall. In semiarid to humid climates (warm temperate shown here [Post *et al.*, 1985]), total soil N increases with rainfall and is mostly organic (>99%), reflecting biological activity. In arid to hyperarid climates, total soil N increases with aridity and is mostly inorganic ($\sim 75\%$), reflecting N in atmospheric deposition.

photochemistry, regional transport, and abiotic reactions dominate.

[52] In the driest Atacama Desert soils, the accumulation and preservation of atmospheric N largely overshadows biotic transformations and losses. Similar conditions may be hypothesized for Mars, which has ancient landscapes and persistent dry conditions that are likely to preserve oxidized atmospheric N in soils. Thus, from the perspective of the N cycle, the Atacama Desert is like few other areas on Earth, but provides a useful analog for understanding processes that may contribute to the surficial geochemistry of Mars over time.

[53] **Acknowledgments.** Funding for this work was provided by NASA-Ames and NSF (R. A.), NASA GSRP and UC Dissertation Year fellowships (S. E.), NASA ASTEP, and NASA NAI (J. L. M.; Penn State Astrobiology Research Center). We thank M. Kashgarian and staff at CAMS/LLNL; T. Torok for GC analysis of PLFA extracts; K. Warren-Rhodes, B. Sutter, A. Zent, and C. Taylor for sampling; B. Gomez-Silva for field assistance and lab use; P. Brooks for water isotope analysis; and two anonymous reviewers for comments that improved the manuscript.

References

- Amundson, R. (2001), The carbon budget in soils, *Annu. Rev. Earth Planet. Sci.*, *29*, 535–562.
- Amundson, R., A. T. Austin, E. A. G. Schuur, K. Yoo, V. Matzek, C. Kendall, A. Uebersax, D. Brenner, and W. T. Baisden (2003), Global patterns of the isotopic composition of soil and plant nitrogen, *Global Biogeochem. Cycles*, *17*(1), 1031, doi:10.1029/2002GB001903.
- Austin, A. T., and L. Vivanco (2006), Plant litter decomposition in a semi-arid ecosystem controlled by photodegradation, *Nature*, *442*, 555–558, doi:10.1038/nature05038.
- Austin, A. T., L. Yahdjian, J. M. Stark, J. Belnap, A. Porporato, U. Norton, D. A. Ravetta, and S. M. Schaeffer (2004), Water pulses and biogeochemical cycles in arid and semiarid ecosystems, *Oecologia*, *141*(2), 221–235.
- Blake, J. J., D. R. Blake, A. L. Swanson, E. Atlas, F. Flocke, and F. S. Rowland (2003), Latitudinal, vertical and seasonal variations of C₁–C₄ alkyl nitrates in the troposphere over the Pacific Ocean during PEM-Tropics A and B: Oceanic and continental sources, *J. Geophys. Res.*, *108*(D2), 8242, doi:10.1029/2001JD001444.
- Böhlke, J. K., G. E. Erickson, and K. Revesz (1997), Stable isotope evidence for an atmospheric origin of desert nitrate deposits in northern Chile and southern California, USA, *Chem. Geol.*, *136*(1–2), 135–152.
- Booth, M. S., J. M. Stark, and E. Rastetter (2005), Controls on nitrogen cycling in terrestrial ecosystems: A synthetic analysis of literature data, *Ecol. Monogr.*, *75*(2), 139–157.
- Brenner, D. L., R. Amundson, W. T. Baisden, C. Kendall, and J. Harden (2001), Soil N and N-15 variation with time in a California annual grassland ecosystem, *Geochim. Cosmochim. Acta*, *65*(22), 4171–4186.
- Calza, P., E. Pelizzetti, and C. Minero (2005), The fate of organic nitrogen in photocatalysis: An overview, *J. Appl. Electrochem.*, *35*, 665–673.
- Capone, D. G., R. Poppa, B. Flood, and K. H. Nealson (2006), Follow the nitrogen, *Science*, *312*(5774), 708–709.
- Casciotti, K. L., D. M. Sigman, M. G. Hastings, J. K. Böhlke, and A. Hilbert (2002), Measurement of the oxygen isotopic composition of nitrate in seawater and freshwater using the denitrifier method, *Anal. Chem.*, *74*(19), 4905–4912.
- Cleveland, C. C., et al. (1999), Global patterns of terrestrial biological nitrogen (N-2) fixation in natural ecosystems, *Global Biogeochem. Cycles*, *13*(2), 623–645.
- Cornell, S. E., T. D. Jickells, J. N. Cape, A. P. Rowland, and R. A. Duce (2003), Organic nitrogen deposition on land and coastal environments: A review of methods and data, *Atmos. Environ.*, *37*(16), 2173–2191.
- Dahl, E. E., S. A. Yvon-Lewis, and E. S. Saltzman (2005), Saturation anomalies of alkyl nitrates in the tropical Pacific Ocean, *Geophys. Res. Lett.*, *32*, L20817, doi:10.1029/2005GL023896.
- Darwin, C. (1909), *The Voyage of the Beagle*, 468 pp., P. F. Collier, New York.
- Erickson, G. E. (1981), Geology and origin of the Chilean nitrate deposits, *Geol. Soc. Prof. Pap.*, *1188*, 37 pp.
- Ewing, S. A., R. Amundson, W. Yang, B. W. Stewart, C. Kendall, and D. J. DePaolo (2005), Two million years of desert aerosols: evidence for non-biological isotopic fractionation of atmospheric Ca in hyperarid soils of the Atacama Desert, Chile, *Eos Trans. AGU*, *86*(52), Fall Meet. Suppl., Abstract PP34A-08.
- Ewing, S. A., B. Sutter, R. Amundson, J. Owen, K. Nishiizumi, W. Sharp, S. S. Cliff, K. Perry, W. E. Dietrich, and C. P. McKay (2006), A threshold in soil formation at Earth's arid-hyperarid transition, *Geochim. Cosmochim. Acta*, *70*(21), 5293–5322, doi:10.1016/j.gca.2006.08.020.
- Firestone, M. K., and E. A. Davidson (1989), Microbiological basis of NO and N₂O production and consumption in soil, in *Exchange of Trace Gases Between Terrestrial Ecosystems and the Atmosphere*, edited by M. O. Andreae and D. S. Schimel, pp. 7–21, John Wiley, Hoboken, N. J.
- Galloway, J. N., et al. (2004), Nitrogen cycles: Past, present, and future, *Biogeochemistry*, *70*(2), 153–226.
- Guckert, J. B., C. P. Antworth, P. D. Nichols, and D. C. White (1985), Phospholipid, ester-linked fatty-acid profiles as reproducible assays for changes in prokaryotic community structure of estuarine sediments, *FEMS Microbiol. Ecol.*, *31*(3), 147–158.
- Hastings, M. G., D. M. Sigman, and F. Lipschultz (2003), Isotopic evidence for source changes of nitrate in rain at Bermuda, *J. Geophys. Res.*, *108*(D24), 4790, doi:10.1029/2003JD003789.
- Hastings, M. G., E. J. Steig, and D. M. Sigman (2004), Seasonal variations in N and O isotopes of nitrate in snow at Summit, Greenland: Implications for the study of nitrate in snow and ice cores, *J. Geophys. Res.*, *109*, D20306, doi:10.1029/2004JD004991.
- Hoffman, E. J., and R. A. Duce (1974), Organic carbon content of marine aerosols collected on Bermuda, *J. Geophys. Res.*, *79*(30), 4474–4477.
- Holland, E. A., F. J. Dentener, B. H. Braswell, and J. M. Sulzman (1999), Contemporary and pre-industrial global reactive nitrogen budgets, *Biogeochemistry*, *46*(1–3), 7–43.
- Jenny, H. (1941), *Factors of Soil Formation*, McGraw-Hill, New York, London.
- Jenny, H., and C. D. Leonard (1934), Functional relationships between soil properties and rainfall, *Soil Sci.*, *38*, 363–381.
- Macalady, J. L., A. M. S. McMillan, A. F. Dickens, S. C. Tyler, and K. M. Scow (2002), Population dynamics of type I and II methanotrophic bacteria in rice soils, *Environ. Microbiol.*, *4*(3), 148–157.
- Maier, R. M., K. P. Drees, J. W. Neilson, D. A. Henderson, J. Quade, and J. L. Betancourt (2004), Microbial life in the Atacama Desert, *Science*, *306*(5700), 1289.
- Mayer, B., S. M. Bollwerk, T. Mansfeldt, B. Hutter, and J. Veizer (2001), The oxygen isotope composition of nitrate generated by nitrification in acid forest floors, *Geochim. Cosmochim. Acta*, *65*(16), 2743–2756.
- Michalski, G., J. Savarino, J. K. Böhlke, and M. Thiemens (2002), Determination of the total oxygen isotopic composition of nitrate and the calibration of a Delta O-17 nitrate reference material, *Anal. Chem.*, *74*(19), 4989–4993.
- Michalski, G., Z. Scott, M. Kabling, and M. H. Thiemens (2003), First measurements and modeling of Delta O-17 in atmospheric nitrate, *Geophys. Res. Lett.*, *30*(16), 1870, doi:10.1029/2003GL017015.
- Michalski, G., J. K. Böhlke, and M. Thiemens (2004), Long term atmospheric deposition as the source of nitrate and other salts in the Atacama Desert, Chile: New evidence from mass-independent oxygen isotopic compositions, *Geochim. Cosmochim. Acta*, *68*(20), 4023–4038.
- Millennium Ecosystem Assessment (2005), *Ecosystems and Human Well-Being: Desertification Synthesis*, World Resour. Ins., Washington, D. C.
- Moore, J. K., S. C. Doney, D. M. Glover, and I. Y. Fung (2002), Iron cycling and nutrient-limitation patterns in surface waters of the World Ocean, *Deep Sea Res., Part II*, *49*(1–3), 463–507.
- Moore, R. M., and N. V. Blough (2002), A marine source of methyl nitrate, *Geophys. Res. Lett.*, *29*(15), 1737, doi:10.1029/2002GL014989.
- Navarro-Gonzalez, R., et al. (2003), Mars-like soils in the Atacama Desert, Chile, and the dry limit of microbial life, *Science*, *302*(5647), 1018–1021.
- Neff, J. C., E. A. Holland, F. J. Dentener, W. H. McDowell, and K. M. Russell (2002), The origin, composition and rates of organic nitrogen deposition: A missing piece of the nitrogen cycle?, *Biogeochemistry*, *57*(1), 99–136.
- Post, W. M., J. Pastor, P. J. Zinke, and A. G. Stangenberger (1985), Global patterns of soil-nitrogen storage, *Nature*, *317*(6038), 613–616.
- Quinn, R. C., A. P. Zent, F. J. Grunthaler, P. Ehrenfreund, C. L. Taylor, and J. R. C. Garry (2005), Detection and characterization of oxidizing acids in the Atacama Desert using the Mars Oxidation Instrument, *Planet. Space Sci.*, *53*(13), 1376–1388.
- Rech, J. A., J. Quade, and W. S. Hart (2003), Isotopic evidence for the source of Ca and S in soil gypsum, anhydrite and calcite in the Atacama Desert, Chile, *Geochim. Cosmochim. Acta*, *67*(4), 575–586.

- Rech, J. A., B. S. Currie, G. Michalski, and A. M. Cowan (2006), Neogene climate change and uplift in the Atacama Desert, Chile, *Geology*, *34*(9), 761–764.
- Reheis, M. C., and R. Kihl (1995), Dust deposition in southern Nevada and California, 1984–1989: Relations to climate, source area, and source lithology, *J. Geophys. Res.*, *100*(D5), 8893–8918.
- Schaeffer, S. M., and R. D. Evans (2005), Pulse additions of soil carbon and nitrogen affect soil nitrogen dynamics in an arid Colorado Plateau shrubland, *Oecologia*, *145*(3), 425–433.
- Schauer, J. J., et al. (2003), ACE-Asia intercomparison of a thermal-optical method for the determination of particle-phase organic and elemental carbon, *Environ. Sci. Technol.*, *37*(5), 993–1001.
- Schlesinger, W. H., and W. T. Peterjohn (1991), Processes controlling ammonia volatilization from Chihuahuan desert soils, *Soil Biol. Biochem.*, *23*(7), 637–642.
- Segura, A., and R. Navarro-González (2005), Nitrogen fixation on early Mars by volcanic lightning and other sources, *Geophys. Res. Lett.*, *32*(5), L05203, doi:10.1029/2004GL021910.
- Sigman, D. M., K. L. Casciotti, M. Andreani, C. Barford, M. Galanter, and J. K. Bohlke (2001), A bacterial method for the nitrogen isotopic analysis of nitrate in seawater and freshwater, *Anal. Chem.*, *73*(17), 4145–4153.
- Stark, J. M., D. R. Smart, S. C. Hart, and K. A. Haubensak (2002), Regulation of nitric oxide emissions from forest and rangeland soils of western North America, *Ecology*, *83*(8), 2278–2292.
- Sylvia, D. M., J. J. Fuhrmann, P. G. Hartel, and D. A. Zuberer (1998), *Principles and Applications of Soil Microbiology*, 550 pp., Prentice-Hall, Upper Saddle River, N. J.
- Trumbore, S. (2000), Age of soil organic matter and soil respiration: Radiocarbon constraints on belowground C dynamics, *Ecol. Appl.*, *10*(2), 399–411.
- Vogel, J. S., J. R. Southon, D. E. Nelson, and T. A. Brown (1984), Performance of catalytically condensed carbon for use in accelerator mass spectrometry, *Nucl. Instrum. Methods Phys. Res.*, *233*(2), 289–293.
- Vuille, M., R. S. Bradley, M. Werner, R. Healy, and F. Keimig (2003), Modeling $\delta^{18}\text{O}$ in precipitation over the tropical Americas: 1. Interannual variability and climatic controls, *J. Geophys. Res.*, *108*(D6), 4174, doi:10.1029/2001JD002038.
- Walvoord, M. A., F. M. Phillips, D. A. Stonestrom, R. D. Evans, P. C. Hartsough, B. D. Newman, and R. G. Striagl (2003), A reservoir of nitrate beneath desert soils, *Science*, *302*(5647), 1021–1024.
- Warren-Rhodes, K., K. L. Rhodes, S. B. Pointing, S. Ewing, D. C. Lacap, B. Gómez-Silva, R. Amundson, E. I. Friedmann, and C. P. McKay (2006), The influence of water availability on cyanobacterial community ecology and the dry limit to photosynthetic life in the Atacama Desert, Chile, *Microb. Ecol.*, *52*, 389–398, doi:10.1007/s00248-006-9055-7.
- West, A. G., S. J. Patrickson, and J. R. Ehleringer (2006), Water extraction times for plant and soil materials used in stable isotope analysis, *Rapid Commun. Mass Spectrom.*, *20*, 1317–1321.
- Zhang, Q., and C. Anastasio (2003), Conversion of fogwater and aerosol organic nitrogen to ammonium, nitrate, and NO_x during exposure to simulated sunlight and ozone, *Environ. Sci. Technol.*, *37*(16), 3522–3530.
- R. Amundson, Division of Ecosystem Sciences, Department of Environmental Science Policy and Management, 137 Mulford Hall, 3114, University of California, Berkeley, CA 94720, USA. (earthyn@nature.berkeley.edu)
- S. A. Ewing, Center for Isotope Geochemistry, Department of Earth and Planetary Science, 4767, University of California, Berkeley, Berkeley, CA 94720-4767, USA. (saewing@nature.berkeley.edu)
- C. Kendall, USGS, 345 Middlefield Road, MS 434, Menlo Park, CA 94025, 94025, USA. (ckendall@usgs.gov)
- S. Kohl, Division of Atmospheric Sciences, Desert Research Institute, 2215 Raggio Parkway, Reno, NV 89512-1095, USA. (steve.kohl@dri.edu)
- J. L. Macalady, Penn State Astrobiology Research Center, Department of Geosciences, Pennsylvania State University, 210 Deike Building, University Park, PA 16802, USA. (jmacalad@geosc.psu.edu)
- C. P. McKay, NASA-Ames Research Center, MS 245-3, Moffett Field, CA 94035, USA. (cmckay@mail.arc.nasa.gov)
- G. Michalski, Department of Earth and Atmospheric Sciences, Purdue University, 550 Stadium Mall Drive, CIVL3229, West Lafayette, IN 47907, USA. (gmichals@purdue.edu)
- R. C. Quinn, SETI Institute, NASA Ames Research Center, MS 239-12, Moffett Field, CA 94035, USA. (rquinn@mail.arc.nasa.gov)
- M. Thieme, Division of Physical Sciences, University of California, San Diego, 9500 Gilman Drive, 0356, La Jolla, CA 92093-0356, USA. (mthiemens@ucsd.edu)
- S. D. Wankel, Department of Organismal and Evolutionary Biology, Harvard University, Biology Labs, Room 3092, 16 Divinity Avenue, Cambridge, MA 02138, USA. (swankel@oeb.harvard.edu)